Electrical and mechanical properties of oriented poly(3-alkylthiophenes): 2. Effect of side-chain length

Jeff Moulton and Paul Smith*
Materials Department, University of California at Santa Barbara, Santa Barbara, CA 93106, USA
(Received 26 March 1991; accepted 16 April 1991)

The mechanical and electrical properties of solution-processed poly(3-alkylthiophenes) with alkyl side-chain lengths of 6, 8 and 12 carbon atoms are discussed. Tensile drawing at elevated temperatures yielded oriented materials with moderately increased mechanical properties. A simple model accounting for defects in the regiospecificity, i.e. head-to-tail *versus* head-to-head or tail-to-tail monomer coupling, is introduced, in addition to side-chain dilution, to account for the low moduli of undoped samples. Doping with $FeCl_3 \cdot 6H_2O$ led to significant enhancement of the mechanical properties of the drawn samples, as well as to high electrical conductivity. As was previously found for other conducting polymer systems, strong correlations were observed between mechanical properties and electrical conductivity. The conductivity was found to scale linearly with tenacity, independent of side-chain length.

(Keywords: poly(3-alkylthiophenes); regiospecificity; electrical conductivity; tensile modulus)

INTRODUCTION

With the introduction of the poly(3-alkylthiophenes), increased processability has allowed for the formation of films and fibres of the polythiophene class of conducting polymers through both melt- and solution-processing routes. Considerable efforts have been devoted to improving the polymer synthesis[1–4] and to investigating the electrical and optical properties as a function of the alkyl side-chain length[5,6].

There has been, however, less research activity directed towards understanding the mechanical properties of this class of processable conducting polymers, compared to the more extensive work on polyacetylene[7], poly(2,5-dimethoxy-*p*-phenylene vinylene)[8] (PDMPV), poly(2,5-thienylene vinylene)[9] (PTV) and poly(phenylene vinylene)[10] (PPV).

This paper is the second part of a broad, systematic study of the electrical conductivity and mechanical properties of the poly(3-alkylthiophenes), and their interdependences. In the present work we examine the effects of the side-chain length on these properties. Chemically prepared[2] poly(3-hexylthiophene) (P3HT), poly(3-octylthiophene) (P3OT) and poly(3-dodecylthiophene) (P3DDT) were used. The characteristics of these substituted polythiophenes were compared with those of electrochemically prepared, unsubstituted polythiophene from Ito *et al.*[11].

The excellent solubility of poly(3-alkylthiophenes) (P3ATs) in a variety of solvents allows one to prepare both films and fibres via a simple solution-processing route at room temperature. This technique avoids complications due to crosslinking, which can occur at processing temperatures above the melting point. Orientation of the alkythiophene macromolecules was introduced through tensile drawing of films and fibres at elevated temperature. The effects of orientation on both the mechanical and electrical properties were determined.

Although tensile drawing improved the stiffness of the (undoped) P3AT filaments, the properties fell far short of those for drawn polythiophene[11]. Wide-angle X-ray diffraction was consistent with a planar stacking of the macromolecules in the crystal structure, but cross-sectional dilution of the unit cell could not fully account for the reduced stiffness. We introduce a simple model that considers both cross-sectional dilution and regiospecific coupling defects, which is shown to account accurately for the stiffness of drawn P3ATs.

In addition to tensile drawing, acceptor doping was also effective in increasing the mechanical properties, as reported elsewhere[12] for P3OT. Finally, a linear correlation was found between electrical conductivity and tenacity, independent of side-chain length.

EXPERIMENTAL METHODS AND TECHNIQUES

Materials

Three poly(3-alkylthiophenes) were used in this study; all materials were synthesized using $FeCl_3$ as a coupling agent[2]. Poly(3-hexylthiophene) and poly(3-dodecylthiophene) samples were kindly supplied by Professor F. Wudl and poly(3-octylthiophene) was provided by Dr J.-E. Österholm by Neste Oy (Finland). Physical characteristics of the P3ATs are listed in *Table 1*. Gel permeation chromatography and measurement of intrinsic viscosities were carried out in $CHCl_3$ at 25°C.

* Department of Chemical and Nuclear Engineering

0032-3861/92/112340-08

Table 1 Physical properties of poly(3-alkylthiophenes)

Sample	$\bar{M}_n$	Polydispersity ($\bar{M}_w/\bar{M}_n$)	Intrinsic viscosity (dl g^{-1})
P3HT	51000	2.2	0.91
P3OT	45000	4.2	1.05
P3DDT	37000	3.2	0.65

Film casting and fibre spinning

Poly(3-alkylthiophenes) were dissolved at room temperature in chloroform and subsequently filtered through 0.2 μm Teflon® filters. Films of filtered P3AT were prepared by casting a 3 wt% polymer solution in chloroform onto a glass surface. The solvent was slowly evaporated under a nitrogen blanket. The resulting films were vacuum dried, at room temperature, for 24 h. This procedure yielded red films of approximately 30–50 μm thickness.

Spinning solutions of prefiltered P3AT were prepared at a polymer concentration of 10 wt% in chloroform. The solutions were wet spun into acetone using a high-precision syringe pump (Sage Instruments, model 355). The viscous solutions were pumped at a rate of 0.19 ml min^{-1} through a spinnerette with a diameter of 0.4 mm. No drawdown was applied during the spinning process. The wet-spun filaments were wound onto a bobbin directly from the coagulation bath and subsequently dried under vacuum for 24 h. Dark red fibres with a linear density of approximately 100 denier were obtained.

Drawing and cross-section determinations

Initial determinations of the maximum draw ratios (λ_{max}) at various temperatures were made with solution-cast films using an Instron Tensile Tester, model 1122, with an attached oven and controller, Instron model 3116. The sample gauge lengths were 20 mm, and the cross-head speed was 20 mm min^{-1}.

Drawing of the dried fibres was carried out in a temperature-controlled, continuous drawing tube furnace with a heated zone length of 12 cm. The temperature of the tube furnace was controlled with an Omega CN-2020 programmable temperature controller. Drawing was carried out at 100 and 105°C in both air and nitrogen atmospheres for P3DDT and P3OT respectively. P3HT was drawn at 140°C in nitrogen. The draw ratios were varied by changing the relative speeds of the feed and take-up spools at either end of the heated tube. The speed of the feed spool was varied from 3.0 to 6.4 cm min^{-1} while the take-up was varied from 8.6 to 31.6 cm min^{-1}, depending on the desired draw ratio.

Cross-sections were determined from each fibre's linear density and specific gravity. The latter was determined by the flotation technique, using water/ethylene glycol solutions for undoped filaments and water/sucrose solutions for $FeCl_3$-doped samples. The densities of undoped filaments were 1.03, 1.05 and 1.11 g cm^{-3} for P3DDT, P3OT and P3HT, respectively. These values were consistent with those of free-standing cast films. Densities of doped fibres were approximately 1.12, 1.18 and 1.25 g cm^{-3} for P3DDT, P3OT and P3HT, respectively.

Characterization and measurement techniques

Tensile properties of doped and undoped fibres were determined with the Instron Tensile Tester at room temperature at a rate of elongation of 100% min^{-1}. Sample gauge lengths were 10 mm. The maximum modulus[12] (E), elongation at break (ε) and strength (σ) were measured and reported as the average of at least three measurements.

Differential scanning calorimetry was carried out with a Mettler DSC 30 calorimetry head and the corresponding Mettler TC 10A controller. All measurements were carried out in nitrogen, and heating rates were 10°C min^{-1}.

Proton n.m.r. spectra were collected with a GE GN 500, 500 MHz, instrument. Polymer solutions were $\approx$1.0 wt% P3AT in $CDCl_3$, with a tetramethylsilane (TMS) reference.

Wide-angle X-ray diffraction (WAXD) patterns were collected using a Philips PW 1729 X-ray generator equipped with a flat-film camera. The radiation was Ni-filtered Cu K_α, generated at 40 mA and 30 kV. Film exposure times varied from 10 to 24 h. The sample-to-film distance was calibrated with Si power.

Iron chloride doping was carried out in solutions of 1 M $FeCl_3 \cdot 6H_2O$/nitromethane, rather than using the anhydrous salt. This doping procedure was used to reduce reported sample brittleness associated with anhydrous $FeCl_3$ doping[13]. Fibres were unconstrained during doping. Conductivity measurements were made with the standard four-point probe technique.

RESULTS AND DISCUSSION

Tensile deformation

The maximum draw ratio *versus* temperature was determined in air for each of the poly(3-alkylthiophenes) at a rate of elongation of 100% min^{-1}. *Figure 1a* shows that, as the side-chain length decreased, increasing temperature was required to achieve the maximum draw ratio, which is consistent with the increasing melting temperatures, shown in *Figure 1b* (cf. also ref. 14). The maximum draw ratios were relatively low owing to the modest molecular weights of the polymers.

Both P3OT and P3DDT showed evidence of molecular relaxation in the most highly drawn samples, whereas P3HT appeared to draw affinely to all draw ratios. This was inferred from thermal shrinkage measurements, which were carried out by placing the drawn samples into a silicone oil bath at 20°C above their melting point. The non-affinely drawn samples did not retract to their original dimensions as the deformation and chain extension processes were accompanied by chain relaxation. The increase in molecular slippage with increased side-chain length is not completely unexpected, in view of the trends observed for the optimum deformation temperature, $T_{\lambda_{max}}$, and the melting point, T_m. A comparison of *Figures 1a* and *1b* shows that the difference between T_m and $T_{\lambda_{max}}$ decreased with increasing side-chain length. Thus, P3ATs with longer side chains were drawn at temperatures approaching the melting point of the polymer, where molecular relaxation becomes significantly more rapid.

Wide-angle X-ray diffraction (WAXD) patterns, nevertheless, indicated that the drawn samples were relatively well oriented, as was inferred from the intense equatorial reflections and well defined layer lines. The WAXD

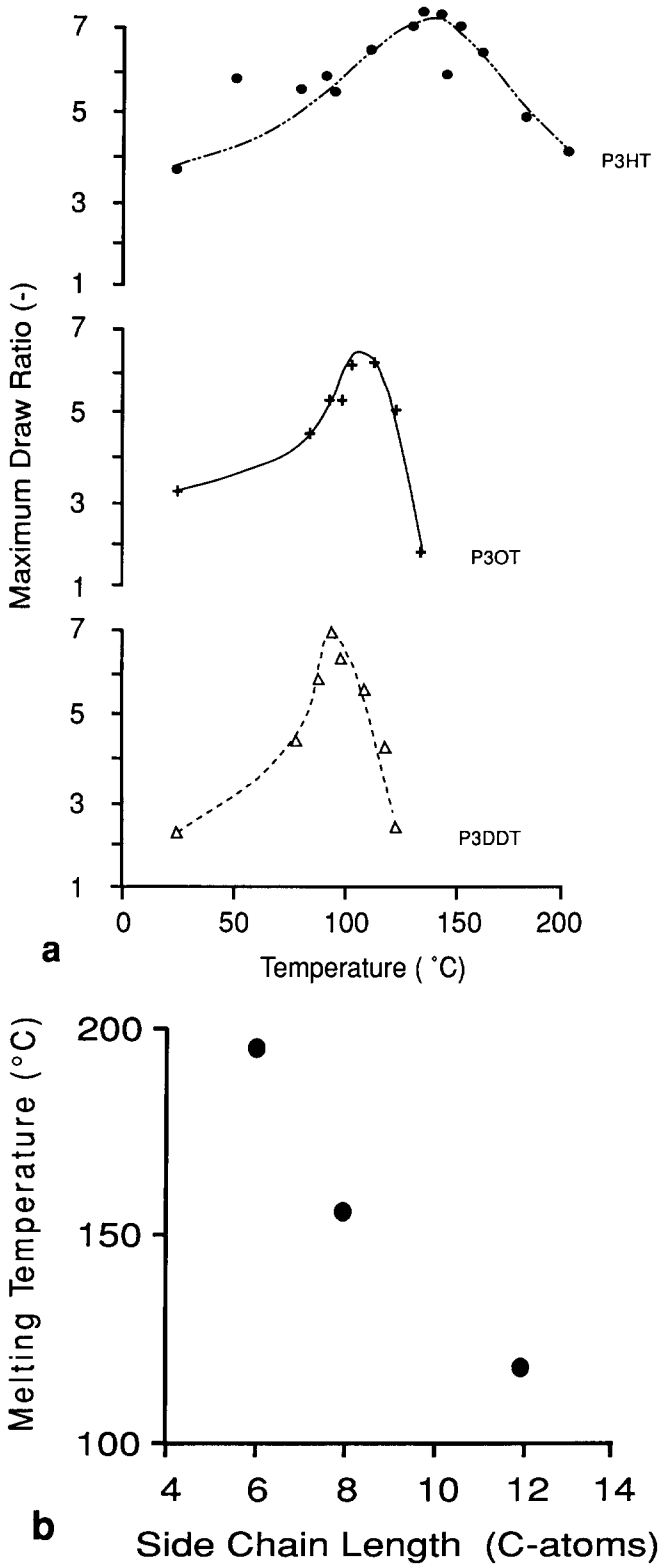

Figure 1 (a) Maximum draw ratio (λ_{max}) *versus* temperature for P3ATs. (b) P3AT melting point *versus* side-chain length (cf. ref. 14)

patterns did, however, show relatively intense amorphous haloes, even in the most highly drawn samples, indicating that substantial internal disorder was still present. Characteristic WAXD fibre patterns of drawn P3HT and P3DDT are shown in *Figure 2*. The P3AT as-spun filaments had heats of fusion in the range of 8 to 10 J g^{-1}, as was determined by differential scanning calorimetry. All of the melting endotherms were broad, of the order of 70°C, and there did not appear to be appreciable side-chain crystallization in the P3DDT sample. Chain alignment and extension did not lead to the observation of any substantial increases in the enthalpy of fusion of the polymers.

The WAXD patterns revealed that the only significant difference in lattice dimension among the various, undoped P3ATs was along the *a* axis. Consistent with previously determined structures[15] and polythiophene repeat periods[16], the *a* axis increased with side-chain length, while both the *b* and *c* axes remained constant throughout the series (see *Table 2*). These data also show that deviation from the linear relationship between the *a* axis dimension and side-chain length occurred at more than eight carbon atoms. The P3DDT sample showed a decreased *a* dimension increment for additional methylenes when compared with both P3HT and P3OT.

Mechanical properties

As observed for most polymers, the elastic modulus and strength, or tenacity, of the P3AT fibres increased with draw ratio. There was also a commensurate decrease in elongation to break with increasing draw ratio. The enhancement of the mechanical properties was not, however, exemplary. The strength and stiffness for drawn, undoped, P3ATs were considerably lower than those of oriented, unsubstituted polythiophene (*Figure 3*). The latter data were taken from Ito *et al.*[11].

Comparable trends were observed from soluble poly(alkyl isocyanates)[17], where increases in alkyl side-chain length led to decreases in both the stiffness and strength. This is due to both a dilution, by the alkyl groups, of the number of load-bearing covalent bonds per unit cross-section and reduced secondary interactions between the main chains[18]. Based on the crystal lattice dimensions determined for the P3ATs, the fraction of the main-chain cross-sectional areas per macromolecule are 0.28 for P3HT, 0.25 for P3OT and 0.20 for P3DDT. This simple correction cannot, however, fully account for the severe reductions in the mechanical properties of the P3ATs when compared with unsubstituted polythiophene[11] (cf. *Figure 5* and discussion below).

An important contribution to the stiffness of conjugated polymers not included in the simple cross-sectional area correction is the effective secondary bond strength due to variable interchain π–π overlap. Leclerc *et al.*[19] have shown that both electrochemically and chemically prepared P3ATs are not only composed of regular head-to-tail (H–T) couplings, but may contain considerable fractions of head-to-head (H–H) and tail-to-tail (T–T) defects. These regiospecific defects may, of course, severely disrupt the aromatic overlap between neighbouring thiophene rings, as shown by Souto Maior *et al.*[20]. These authors demonstrated that polymer stereoregularity, achieved through the polymerization of 3,3′-dialkyl-2,2′-bithiophenes, significantly affects the position of the

Table 2 Unit-cell dimensions undoped poly(3-alkylthiophenes)[a]

Sample	*a*/2 (Å)	*b*/2 (Å)	*c* (Å)
P3HT	17.4	3.9	7.8
P3OT	21.1	4.0	7.8
P3DDT	27.0	3.9	7.9

[a]The values of *a*/2 and *b*/2 are the experimentally determined interlayer spacings. The *trans* nature of the P3AT backbones requires a doubling of both of these values in describing the overall unit-cell dimensions

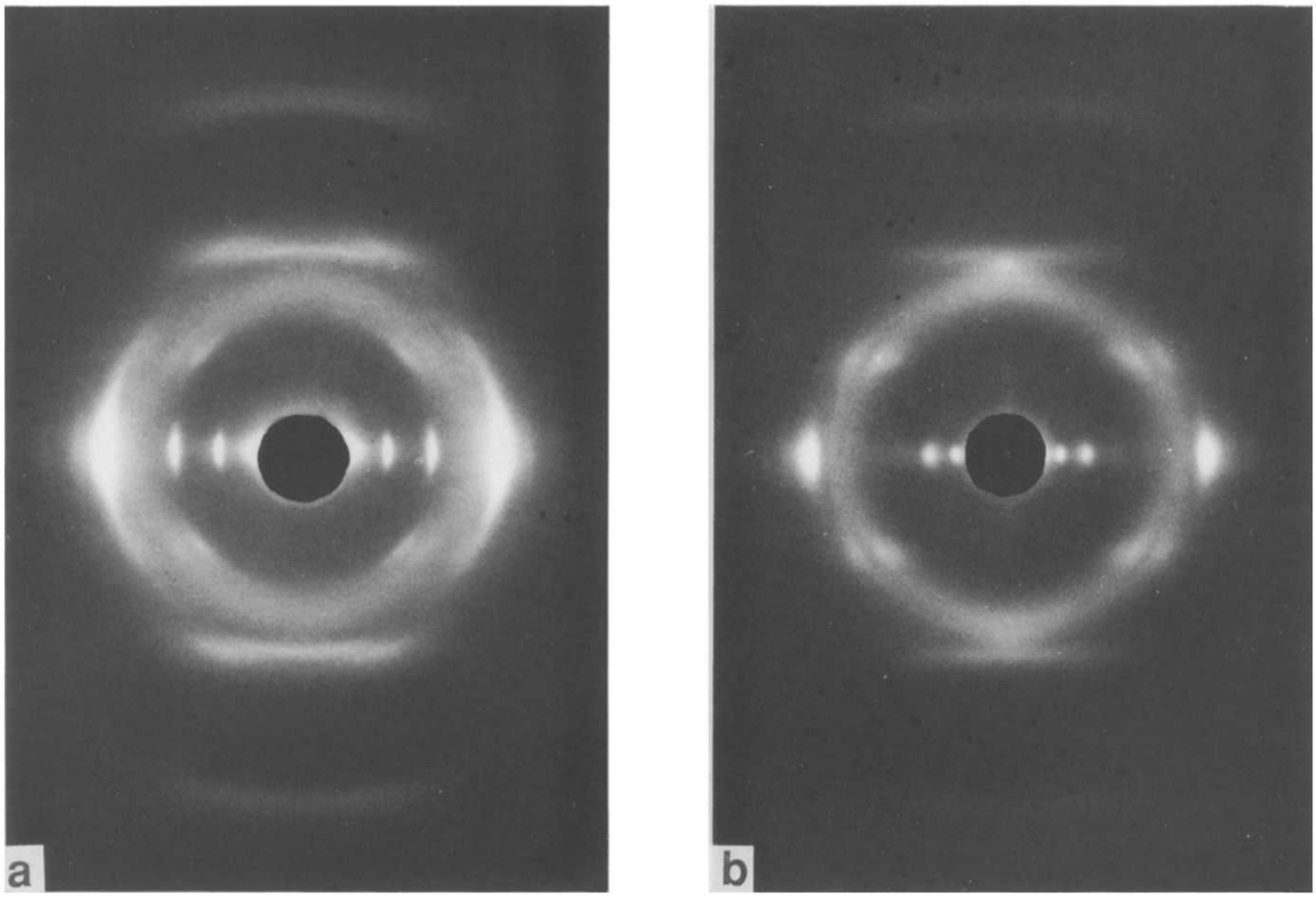

Figure 2 WAXD fibre patterns of (a) drawn P3HT and (b) P3DDT, $\lambda \approx 4.5$. The fibre direction is vertical

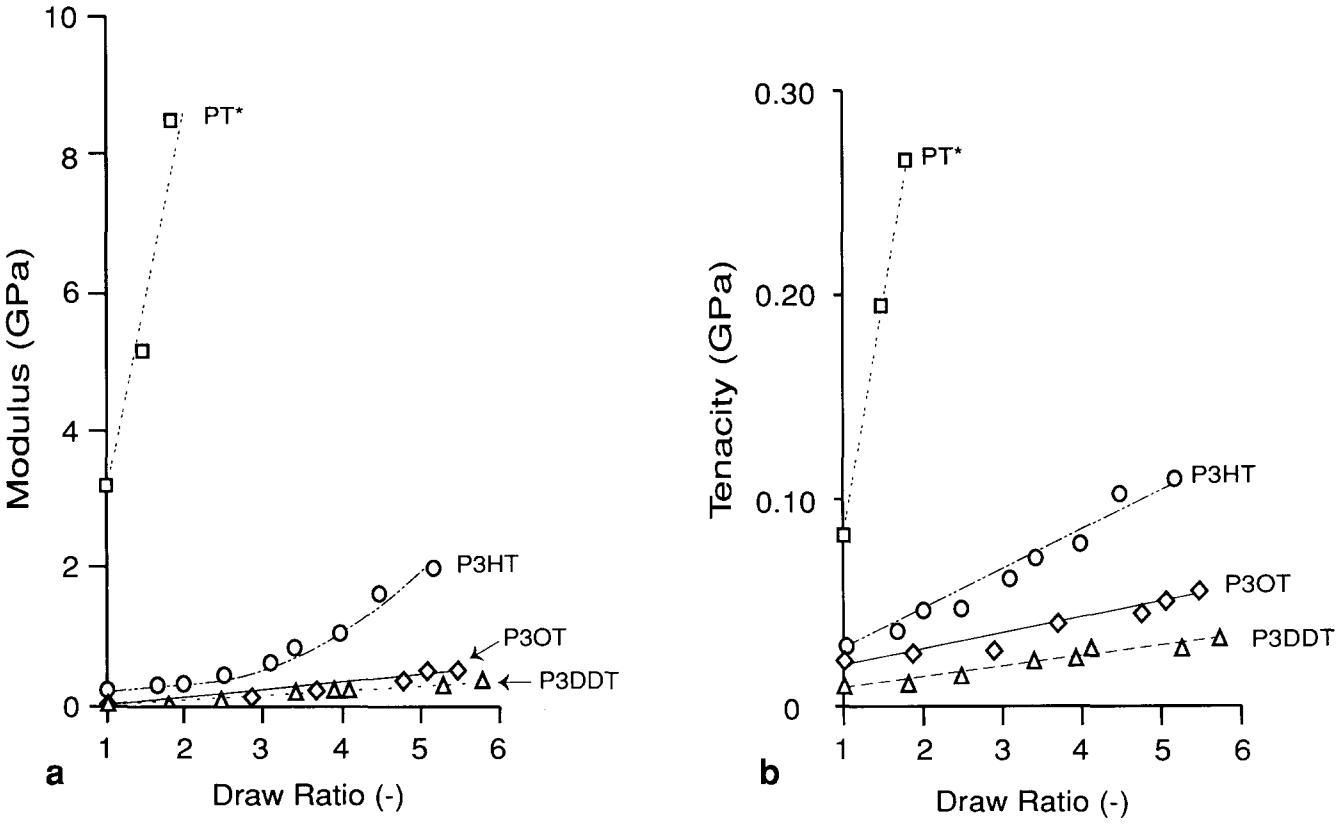

Figure 3 Mechanical properties, i.e. (a) Young's modulus and (b) tenacity, *versus* draw ratio for undoped polythiophenes: (□) PT, (○) P3HT, (◇) P3OT, (△) P3DDT (*unsubstituted polythiophene data from ref. 11)

visible absorption maximum. Regiospecific (H–H) alkylthiophenes were found to absorb with peak maxima of approximately 100 nm shorter wavelength than the monosubstituted derivatives with both head-to-tail and head-to-head couplings. This reduction in the wavelength of the absorption maximum was shown to be due to defect-induced non-coplanarity of the regiospecific H–H polymers.

Following the assignment by Elsenbaumer *et al.*[21] of the 2.8 ppm shift in ^{1}H n.m.r. to H–T coupling, we determined that polymerization resulted in configurations of approximately 80% H–T for P3HT and 75% for P3OT and P3DDT. It is well known[22] that even low degrees of miscoupling may effectively disrupt crystallinity. Crystallographic disruption, of course, affects the secondary bond overlap through torsional defects within the backbone.

As an attempt to account for the effect of the regiospecific defects in the reduction of stiffness, we have modelled the undoped P3AT backbones as aromatic units connected through freely rotating σ bonds, schematically shown in *Figure 4*. The modulus (E) is calculated using the following expression:

$$E = E_{PT} A R^n \qquad (1)$$

where E_{PT} is the modulus of the unsubstituted polythiophene, which was estimated by a linear extrapolation of the data of Ito *et al.*[11]. (Note that the extrapolated value of $E_{PT} \approx 35$ GPa at a draw ratio of 6.) In equation (1), A denotes the ratio between the cross-sectional areas of polythiophene and the poly(3-alkylthiophene) chains, and accounts for side-chain dilution of the main chain within the unit cell (*Table 2*). R equals the fraction of head-to-tail couplings, approximately 0.80 for P3HT and 0.75 for P3OT and P3DDT. Finally, the exponent n is the number of H–T σ bonds surrounding, and resulting

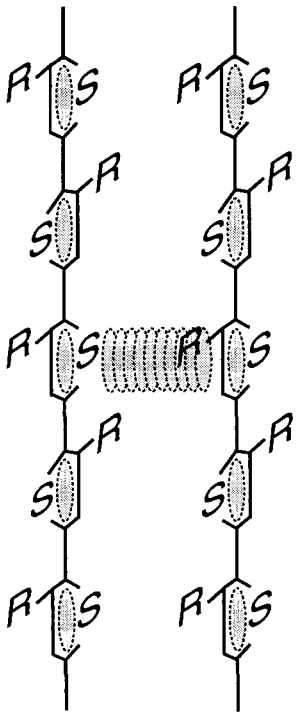

Figure 4 Schematic diagram of effective π–π overlap between neighbouring thiophene rings surrounded by all head-to-tail couplings

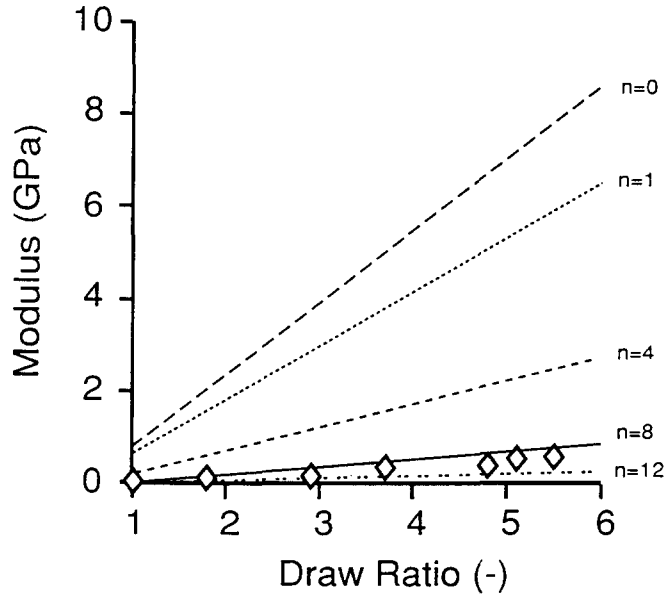

Figure 5 Moduli for undoped P3OT calculated with equation (1) ($R = 0.73$) and various values of n; (◇) data of *Figure 3a*

in, an effective π bond between neighbouring thiophene rings. If we assume a simple symmetric model, then the values of n are likely to be close to, if not equal to, multiples of 4, as a single π–π bond is surrounded by four σ bonds (see *Figure 4*). Simple probability arguments show that R^n will equal the total fraction of *effective* π–π bonds, i.e. those contributing to the stiffness.

Combining the effects of both cross-sectional dilution and main-chain miscouplings, we have determined an effective defect length, i.e. the number of bonds beyond a coupling mismatch through which aromatic overlap is disrupted. Neither cross-sectional dilution alone ($n = 0$) nor combination with a simple fractional accounting ($n = 1$) of the miscoupling will account for the very low moduli of the undoped filaments. The best fit between calculated moduli and experimental data for undoped P3OT (*Figure 5*) suggests that a single aromatic secondary bond may be disrupted if one of the eight adjacent σ bonds are miscoupled. Therefore, any coupling defect randomly placed along the backbone will also affect the two adjacent σ bonds, which is a relatively modest perturbation. *Figure 6* shows that the elastic modulus of all three of the P3ATs can be qualitatively modelled through the use of equation (1) with $n = 8$.

As we have shown elsewhere for poly(3-octylthiophene)[12], the P3ATs exhibit increases in both the stiffness and strength after doping, in addition to becoming electrically conductive. Doping increased the modulus up to an order of magnitude for isotropic samples, while drawn materials showed increases of 2–5 times. The tenacity of P3HT remained constant, but both P3OT and P3DDT showed a doubling in strength after $FeCl_3$ doping. The stiffness and strength of the doped materials are shown, as a function of draw ratio, in *Figures 7a* and *7b*, respectively. The dopant levels were ~0.2 when calculated in terms of $FeCl_4^-$ vs. monomer.

The increases in stiffness with doping may, perhaps, be understood in light of the high percentage of coupling defects. It is well known that doping introduces regions of quinoidal structure (bipolarons) into the P3ATs. A requirement of this structure is the formation of double

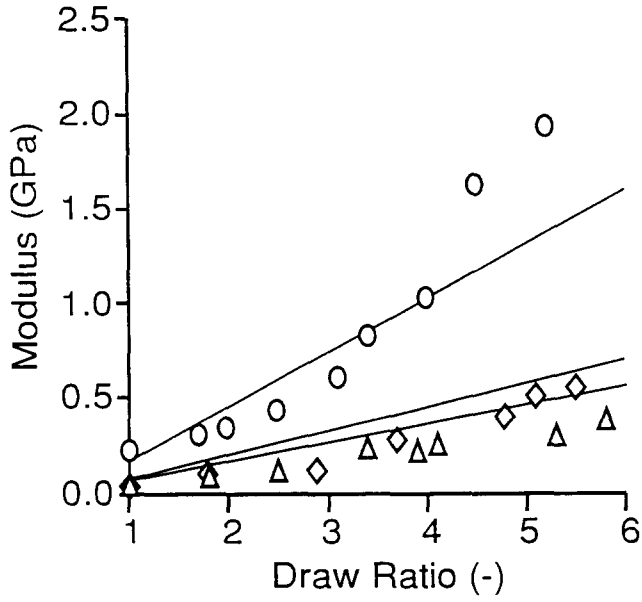

Figure 6 Calculated and experimental moduli for undoped P3ATs: full lines have been calculated using equation (1); (○) P3HT, (◇) P3OT, (△) P3DDT

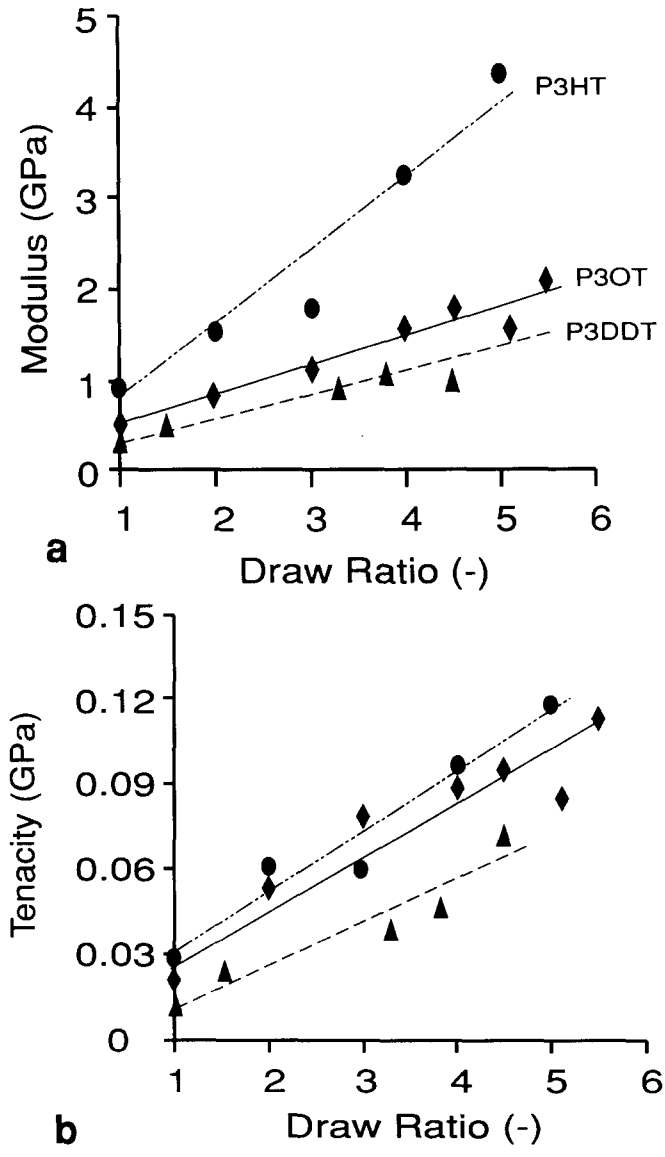

Figure 7 Mechanical properties, i.e. (a) elastic modulus and (b) tenacity, *versus* draw ratio for P3ATs doped with $FeCl_3 \cdot 6H_2O$: (●) P3HT, (◆) P3OT, (▲) P3DDT

bonds along the backbone, thereby removing much of the free rotation inherent to the undoped samples and greatly increasing the coherence length[23]. The conformational changes, occurring due to the rearrangement of aromatic electrons, may not completely remove the effects of miscoupling, but they may limit the extent to which the distortions affect neighbouring bonds. Application of equation (1) is effective in predicting the stiffness of doped filaments if the exponent n is reduced from 8 to 4 (see *Figure 8*). The reduction in n indicates that the doping process has, in fact, increased the effective contribution of π–π overlap to the overall stiffness.

The side-chain length also had a significant effect on the relative changes in stiffness with doping, i.e. the increase in doped modulus to undoped modulus at constant draw ratio. P3DDT showed the larger change, while P3HT showed the least. A plot of the relative slopes of modulus–draw ratio plots $(dE_{doped}/d\lambda)/(dE_{undoped}/d\lambda)$ vs. side-chain length extrapolates to approximately 1 (see *Figure 9*), indicating that there should not be a significant

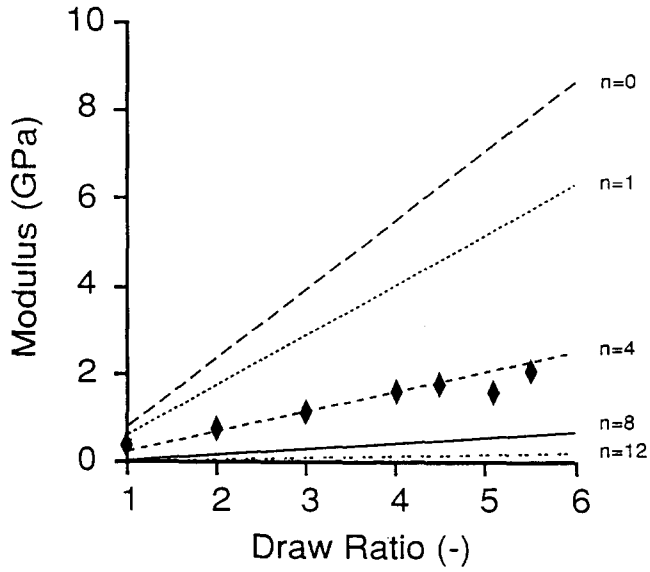

Figure 8 Moduli for doped P3OT calculated with equation (1) ($R = 0.73$) and various values of n; (◆) data of *Figure 7a*

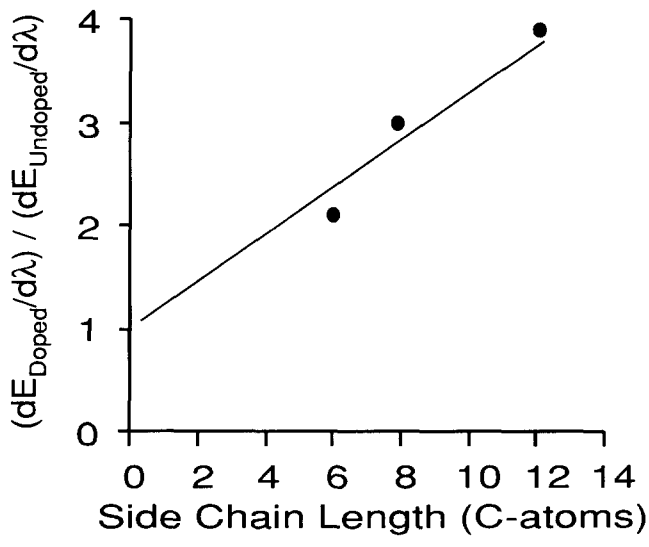

Figure 9 Ratio of the change in modulus *versus* draw ratio slope for both undoped and $FeCl_3 \cdot 6H_2O$-doped P3ATs as a function of side-chain length

change in stiffness upon doping unsubstituted polythiophene. This is in gratifying accord with observations by Ito *et al.*[11].

Wide-angle X-ray diffraction of $FeCl_3$-doped P3ATs showed that the *a* axis dimensions increased in all cases, with the largest percentile expansions, ≈19%, seen in P3DDT. P3HT and P3OT showed lateral expansions of 7% and 10% respectively. Commensurate with increases along the *a* axis, all of the samples exhibited decreases in the inter-ring spacing from ≈3.9 Å to ≈3.7 Å. This decrease is consistent with a more planar backbone structure. Lattice dimensions of the doped polymers are listed in *Table 3*.

Electrical properties

Drawing improved the electrical conductivity by factors of 3–5 for moderately doped samples, ≈20 mol% $FeCl_4^-$. With the exception of some low conductivity values for P3HT at low draw ratios, the trend in conductivity *versus* draw ratio increased from P3DDT to P3HT as shown in *Figure 10*.

We observed, as before for a variety of other systems[7–9], strong correlations between the electrical conductivity and mechanical properties. In particular, there were linear relationships between the conductivity and modulus of the doped P3ATs. As would be expected, P3DDT, with the lowest fraction of main chain per unit cell cross-section, exhibited the lowest modulus and conductivity, while the highest values were observed for P3HT. More importantly, there was no dependence on side-chain length when the conductivities were compared

Table 3 Unit-cell dimensions of $FeCl_3$-doped poly(3-alkylthiophenes)[a]

Sample	*a*/2 (Å)	*b*/2 (Å)	*c* (Å)
P3HT	18.7	3.7	7.8
P3OT	23.3	3.7	8.0
P3DDT	32.1	3.7	7.9

[a]The values of *a*/2 and *b*/2 are the experimentally determined interlayer spacings. The *trans* nature of the P3AT backbones requires a doubling of both of these values in describing the overall unit-cell dimensions

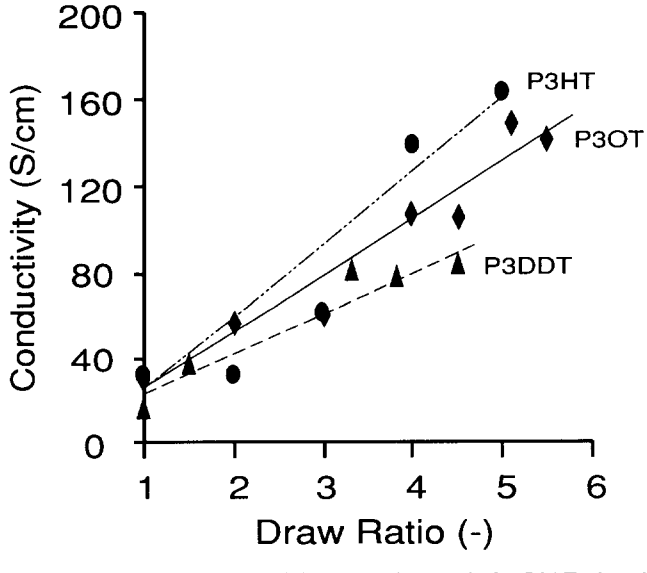

Figure 10 Electrical conductivity *versus* draw ratio for P3ATs doped with $FeCl_3 \cdot 6H_2O$: (●) P3HT, (◆) P3OT, (▲) P3DDT

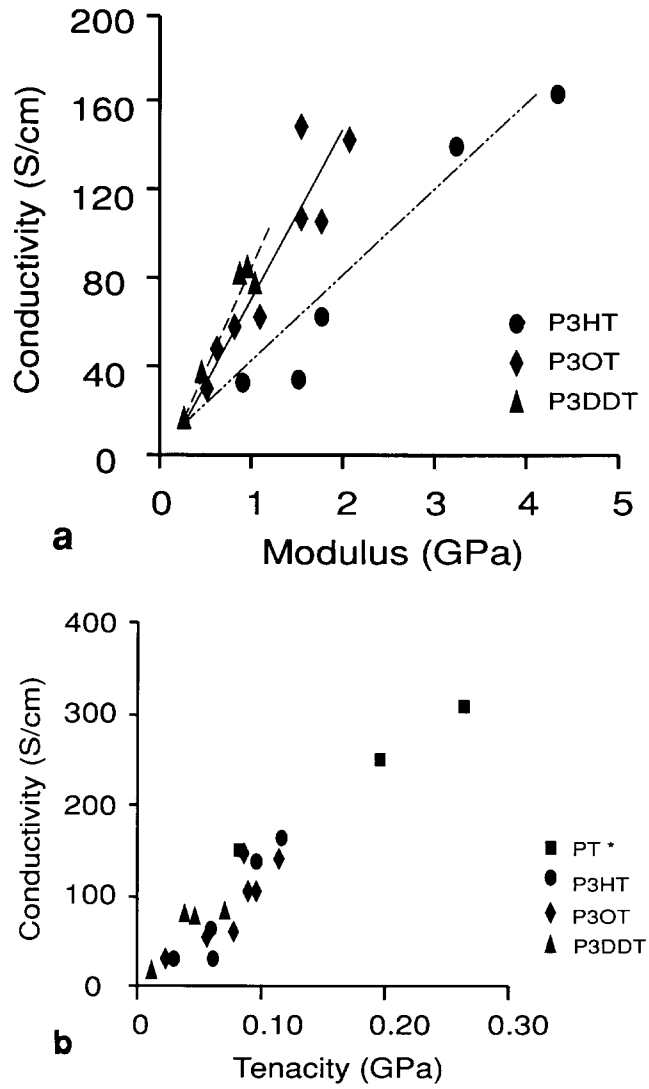

Figure 11 Electrical conductivity *versus* mechanical properties, i.e. (a) conductivity *versus* Young's modulus and (b) conductivity *versus* tenacity, for P3ATs doped with $FeCl_3 \cdot 6H_2O$: (■) PT, (●) P3HT, (◆) P3OT, (▲) P3DDT (*unsubstituted thiophene data from ref. 11 for uncompensated electrochemically polymerized samples)

with respect to strength. As a matter of fact, corresponding data for unsubstituted polythiophene[11] were superimposable on those of the P3AT series. The conductivity *versus* modulus and strength are shown in *Figures 11a* and *11b* respectively.

This interesting result is in agreement with and, in fact, supports earlier suggestions[24] that both electrical conductivity and tensile strength are strongly affected by both inter- and intrachain interactions. Therefore, a strong correlation should exist between these two properties. Electrical conductivity in polymer materials of finite chain length requires both inter- and intrachain electronic mobility for extended electrical transport. Conduction, therefore, requires that the coherence length scales with both the inter- and intrachain electronic transfer mechanisms:

$$L/a \gg (t_0/t_{3d}) \qquad (2)$$

Here L is the coherence length, a the chain repeat unit length, t_0 the intrachain π-electron transfer integral and t_{3d} is the interchain π-electron transfer integral. A similar inequality can be formulated to describe the strength of

polymeric materials:

$$L/a \gg (E_0/E_{3d}) \quad (3)$$

where E_0 is the energy required to break covalent main-chain bonds while E_{3d} represents the energy to break the weaker secondary bonds. L and a are again the coherence length and repeat unit length respectively.

In the case of the tensile strength, the weaker interchain bonds ideally add coherently such that polymers fail through main-chain rupture. Because both the strength and electrical conductivity are strongly dependent on both the main-chain and secondary interactions, one would expect the conductivity to scale linearly with tenacity, as observed.

CONCLUSIONS

The mechanical and electrical properties of three oriented poly(3-alkylthiophenes), of side-chain lengths of 6, 8 and 12 carbons, were compared with the properties of unsubstituted polythiophene[11]. A room-temperature solution-processing route was used to produce films and fibres, thereby avoiding the possibility of crosslinking at temperatures above the melting point. Chain extension of the alkylthiophenes was introduced through tensile drawing at elevated temperature, $T < T_m$.

Although tensile drawing improved the stiffness of the undoped P3AT filaments, the properties fell far short of those for drawn unsubstituted polythiophene. Wide-angle X-ray diffraction of the P3ATs was consistent with a planar arrangement of the macromolecules within the crystal structure, but the relative cross-sectional areas of unsubstituted polythiophene and the poly(3-alkylthiophenes) could not fully explain the modest stiffness. To account for the low values of the modulus, in comparison with unsubstituted polythiophene, we have introduced an expression describing the stiffness in terms of the regiospecificity of monomer coupling, as well as considering side-chain dilution. This model was capable of qualitatively accounting for the stiffness of each of the P3ATs, in both their doped and undoped forms.

In addition to tensile drawing, acceptor doping was also effective in increasing the mechanical properties. When expressed in terms of draw ratio or modulus, the electrical conductivity of doped materials showed a dependence on side-chain length. There was, however, a linear correlation between electrical conductivity and tenacity, independent of side-chain length. This independence was consistent with both the electrical conductivity and strength being strongly dependent on both inter- and intrachain bonding.

ACKNOWLEDGEMENTS

This work was jointly supported by DARPA-AFOSR and monitored by AFOSR under contract number F49620-88-C-0138. The authors would like to thank Dr A. R. Postema for fruitful discussions and Professor A. J. Heeger for critical reading of the manuscript.

REFERENCES

1 Elsenbaumer, R. L., Jen, K. Y. and Oboodi, R. *Synth. Met.* 1986, **15**, 169
2 Sugimoto, R., Takeda, S., Gu, H. B. and Yoshino, K. *Chem. Express* 1986, **1**(11), 635
3 Hotta, S., Soga, M. and Sonoda, N. *Synth. Met.* 1988, **26**, 267
4 Österholm, J.-E., Laakso, J., Nyholm, P., Isotalo, H., Stubb, H., Inganäs, O. and Salaneck, W. R. *Synth. Met.* 1989, **28**, C435
5 Yoshino, K., Nakajima, S., Gu, H. B. and Sugimoto, R. *Japan. J. Appl. Phys.* 1987, **26**(8), L1371
6 Ronacli, J., Garreau, R., Yassar, A., Marque, P., Garnier, F. and Lemaire, M. *J. Phys. Chem.* 1987, **91**, 6706
7 Akagai, K., Suezaki, M., Shirakawa, H., Kyotani, H., Shimamura, M. and Tanabe, Y. *Synth. Met.* 1989, **28**, D1; Cao, Y., Smith, P. and Heeger, A. J. *Polymer* 1991, **32**, 1210
8 Tokito, S., Smith, P. and Heeger, A. J. *Polymer* 1991, **32**, 464
9 Tokito, S., Smith, P. and Heeger, A. J. *Synth. Met.* 1990, **36**, 183
10 Machado, J. M., Masse, M. A. and Karasz, F. E. *Polymer* 1989, **30**, 1992
11 Ito, M., Tsuruno, A., Osawa, S. and Tanaka, K. *Polymer* 1988, **29**, 1161
12 Moulton, J. and Smith, P. *Synth. Met.* 1991, **40**, 13
13 Loponen, M., Neste Oy, private communication
14 Yoshino, K., Nakajima, S., Fujii, M. and Sugimoto, R. *Polym. Commun.* 1987, **28**(11), 309
15 Winokur, M. J., Speigel, D., Kim, Y., Hotta, S. and Heeger, A. J. *Synth. Met.* 1989, **28**, C419
16 Brückner, S. and Porzio, W. *Makromol. Chem.* 1988, **189**, 961
17 Aharoni, S. M. *Polymer* 1981, **22**, 418
18 Postema, A. R., Liou, K., Wudl, F. and Smith, P. *Macromolecules* 1990, **23**, 1842
19 Leclerc, M., Diaz, F. M. and Wegner, G. *Makromol. Chem.* 1989, **190**, 3105
20 Souto Maior, R. M., Hinkelmann, H., Eckert, H. and Wudl, F. *Macromolecules* 1990, **23**, 1268
21 Elsenbaumer, R. L., Jen, K.-Y., Miller, G. G., Eckhardt, H., Shacklette, L. W. and Jow, R. 'Springer Series in Solid State Sciences', Vol. 76, Springer, Berlin, 1987, p. 400
22 Wunderlich, B. 'Macromolecular Physics', Academic Press, New York, 1973
23 Aime, J. P., Bargain, F., Schott, M., Eckhardt, H., Miller, G. G. and Elsenbaumer, R. L. *Phys. Rev. Lett.* 1989, **62**(1), 55
24 Andreatta, A., Tokito, S., Smith, P. and Heeger, A. J. *Mater. Res. Soc. Symp. Proc.* 1990, **173**, 269